iScience

Article

Refined semi-lethal aerosol H5N1 influenza model in cynomolgus macaques for evaluation of medical countermeasures

Macaque model of severe H5N1 influenza

aQIV

Control

Masaru Kanekiyo,
Rebecca A.
Gillespie, Morgan
Midgett, ..., Barney
S. Graham, Simon
M. Barratt-Boyes,
Douglas S. Reed

dsreed@pitt.edu

Highlights

Refined the H5N1 aerosol macaque model of lethal influenza

Lower virus doses did not extend the disease course

Three doses of licensed quadrivalent influenza vaccine plus adjuvant protected against death

Pre-challenge neutralizing antibody titers correlated with protection

Article

Refined semi-lethal aerosol H5N1 influenza model in cynomolgus macaques for evaluation of medical countermeasures

Masaru Kanekiyo,[1,15] Rebecca A. Gillespie,[1] Morgan Midgett,[2] Katherine J. O'Malley,[2,7] Connor Williams,[2] Syed M. Moin,[1] Megan Wallace,[3,8] Luke Treaster,[4] Kristine Cooper,[5] Hubza Syeda,[1] Gwenddolen Kettenburg,[3,9] Hasala Rannulu,[2,10] Tabitha Schmer,[2] Lucia Ortiz,[6] Priscila Da Silva Castanha,[3] Jacqueline Corry,[3,11] Mengying Xia,[2,12] Emily Olsen,[2,13] Daniel Perez,[6] Gabin Yun,[4] Barney S. Graham,[1,14] Simon M. Barratt-Boyes,[3,15] and Douglas S. Reed[2,15,16,*]

SUMMARY

Highly pathogenic avian influenza A H5N1 viruses cause high mortality in humans and have pandemic potential. Effective vaccines and treatments against this threat are urgently needed. Here, we have refined our previously established model of lethal H5N1 infection in cynomolgus macaques. An inhaled aerosol virus dose of 5.1 $\log_{10}$ plaque-forming unit (pfu) induced a strong febrile response and acute respiratory disease, with four out of six macaques succumbing after challenge. Vaccination with three doses of adjuvanted seasonal quadrivalent influenza vaccine elicited low but detectable neutralizing antibody to H5N1. All six vaccinated macaques survived four times the 50% lethal dose of aerosolized H5N1, while four of six unvaccinated controls succumbed to disease. Although vaccination did not protect against severe influenza, vaccinees had reduced respiratory dysfunction and lower viral load in airways compared to controls. We anticipate that our macaque model will play a vital role in evaluating vaccines and antivirals against influenza pandemics.

INTRODUCTION

The ongoing severe acute respiratory syndrome coronavirus 2 (SARS-CoV-2) pandemic has demonstrated the need to have vaccines and countermeasures readily available that can protect against new viruses or bacteria that may emerge and spread rapidly. There have been increasing reports of human cases of influenza caused by avian viruses over the last twenty-five years, particularly among poultry workers.[1,2] In most cases, the disease caused by avian influenza viruses in humans is mild and self-limiting. Highly pathogenic avian influenza (HPAI) H5N1 viruses, in contrast, can cause severe respiratory disease in humans and have a high fatality rate (60%, depending on the outbreak).[1] Influenza viruses can adapt to new hosts or reassort with one another, creating new viruses for which there is little or no pre-existing immunity in the human population. There is significant concern that these highly lethal avian influenza viruses could either adapt to mammalian hosts or reassort with a human seasonal influenza virus, triggering a new pandemic on the scale last seen in 1918 when an estimated 50–100 million (~2.5%–5% of the population) people died worldwide.[3–6] Vaccines and antiviral drugs that can protect against this potential threat are urgently needed. Epidemiological studies have suggested that early-life exposure to human influenza viruses provides immunological imprinting, which may protect against group-related avian influenza viruses later.[7] Similarly, prior exposure of ferrets to H1N1 protected

[1]Molecular Engineering Section, Vaccine Research Center, National Institutes of Health, Bethesda, MD, USA
[2]Center for Vaccine Research, University of Pittsburgh, Pittsburgh, PA, USA
[3]Department of Infectious Disease and Microbiology, University of Pittsburgh, Pittsburgh, PA, USA
[4]Division of Cardiothoracic Imaging, University of Pittsburgh Medical Center, Pittsburgh, PA, USA
[5]Biostatistics Facility, UPMC Hillman Cancer Center, University of Pittsburgh, Pittsburgh, PA, USA
[6]Department of Population Health, University of Georgia, Athens, GA, USA
[7]Present address: WCG Clinical, Inc., Bryn Mawr, PA, USA
[8]Present address: Q2 Lab Solutions, Durham, NC, USA
[9]Present address: University of Chicago, Department of Ecology and Evolution, Chicago, IL, USA
[10]Present address: School of Medicine, Pennsylvania State University, State College, PA, USA
[11]Present address: College of Arts & Sciences, Department of Microbiology, Ohio State University, Columbus, OH, USA
[12]Present address: Drug Discovery Institute, University of Pittsburgh, Pittsburgh, PA, USA
[13]Present address: Department of Microbiology & Immunology, Tulane National Primate Center, Tulane University, Covington, LA, USA
[14]Present address: Department of Medicine and Microbiology, Biochemistry, & Immunology, Morehouse School of Medicine, Atlanta, GA, USA
[15]These authors contributed equally
[16]Lead contact
*Correspondence: dsreed@pitt.edu
https://doi.org/10.1016/j.isci.2023.107830

Table 1. Summary of doses, outcome, and febrile responses after aerosol exposure to H5N1

Animal ID	Weight	Dose[a]	TTD[b]	Fever			
				ΔT Max[c]	Duration[d]	Severity[e]	Ave Elev[f]
147-19	3.9	2.14	15	2.8	78.3	74.1	0.9
148-19	3.8	3.07	15	2.1	73.3	87.6	1.2
153-19	3.2	4.26	15	3.0	109.3	122.5	1.1
154-19	3.2	4.21	15	3.5	123.0	220.0	1.8
156-19	3.8	4.70	15	2.7	206.3	237.1	1.1
145-19	6.4	5.04	4	2.4	87.0	118.4	1.4
150-19	3.1	5.06	6	3.1	108.8	168.5	1.5
155-19	3.2	5.16	15	2.6	153.5	192.6	1.3
151-19	5	5.36	5	2.4	43.0	50.5	1.2
146-19	3.3	5.39	15	2.6	100.5	110.2	1.1
152-19	4.1	5.53	5	3.2	77.5	121.6	1.6

[a]Dose = inhaled dose, in log10 pfu.
[b]TTD = time to death.
[c]ΔTmax = maximum deviation from predicted temperatures.
[d]Duration = hours of significant temperature deviation from predicted.
[e]Severity = sum of significant temperature deviations, adjusted to hours.
[f]Ave Elev = average elevation in temperature, the product of dividing Severity by Duration.

against H5N1 challenge.[8] It is unclear whether vaccination against seasonal human influenza viruses might similarly protect from lethality caused by avian influenza viruses.

Cynomolgus macaques have been used as a model to study severe influenza since the 1997 H5N1 outbreak in Hong Kong.[9] Studies have shown that cynomolgus macaques inoculated with high doses of H5N1 (6.5–7.8 $\log_{10}$ plaque-forming unit [pfu]) via a combination of "mucosal" routes (intranasal, intratracheal, oral, and/or ocular) generally develop mild disease, with only 2 out of 49 macaques succumbing to infection in previous reports.[9–14] Avian influenza viruses, including HPAI viruses, preferentially bind α2,3 sialic acids which in humans are found predominantly in the lower respiratory tract.[15–17] A similar pattern of α2,3 sialic acid expression and H5N1 binding is seen in macaques.[18–20] Inhalation by macaques of H5N1 virus in a small-particle aerosol (<5 μm mass median aerodynamic diameter) similar to a natural respiratory infection should deliver more H5N1 virus to the deep lung and more evenly distribute the virus throughout the lung unlike liquid instillation methods.[21–24] In our previous studies, we found that inhalation of small-particle aerosols containing HPAI H5N1 (A/Vietnam/1203/2004) virus with a dose comparable to what had been given in mucosal inoculations (7.65 $\log_{10}$ pfu) was highly lethal in cynomolgus macaques, with death occurring in 3.6 days.[25] Subsequent macaques received a 10-fold lower dose yet still succumbed in less than 4 days. There was an open question whether the abbreviated disease course and severe outcome after inhalation of aerosolized H5N1 in macaques were a function of the doses used, and whether using lower doses would extend the disease course and alter outcome. A lower dose might be more useful in evaluating potential vaccines or therapeutics as it better reflects natural exposure events.

In this report, we sought to refine the lethal H5N1 infection macaque model to better understand the relationship between inhaled dose and disease course, and to evaluate whether vaccination against seasonal influenza using an adjuvanted quadrivalent influenza vaccine (aQIV) could offer protection from mortality and/or morbidity caused by the HPAI H5N1 infection in macaques.

RESULTS

Refinement of the H5N1 macaque model

Cynomolgus macaques exposed to ~6 $\log_{10}$ pfu of A/Vietnam/1203/2004 H5N1 virus by small-particle aerosol develop acute respiratory distress syndrome (ARDS) and death from 2 to 6 days post-challenge.[25] To assess what impact a lower aerosol H5N1 dose would have on the disease course and outcome, eleven cynomolgus macaques were exposed to varying inhaled doses of H5N1 virus via a small-particle aerosol generated with a vibrating mesh nebulizer using the Aero3G aerosol exposure system in the same fashion as was done previously.[25,26] Aerosol samples were collected during the exposure to determine virus concentration as well as particle size; inhaled dose was calculated as the product of the virus concentration in the aerosol and the total volume of air inhaled by the macaque.[27] Inhaled doses spanned a range of 2.1–5.5 $\log_{10}$ pfu that is 10–10,000 times lower than previously tested doses (Table 1). Regardless of dose, all H5N1-exposed macaques developed a fever response within 24 h after infection (daily median temperature deviations from predicted shown in Figure 1A; actual temperatures shown in Figure S1). None of the five macaques exposed to doses <5 $\log_{10}$ pfu succumbed to infection, nor did they develop ARDS, although there was some sign of mild respiratory disease at the 4–4.9 $\log_{10}$ pfu doses as evidenced by increased respiratory rate, decreased inspiratory time, and decreased expiratory time in two of three macaques (Figures 1B–1D, left and center graphs). At doses between 5 and 5.5 $\log_{10}$ pfu, four of six macaques succumbed between 4 and 6 days post-infection with clinical signs suggesting ARDS. Five of the six macaques
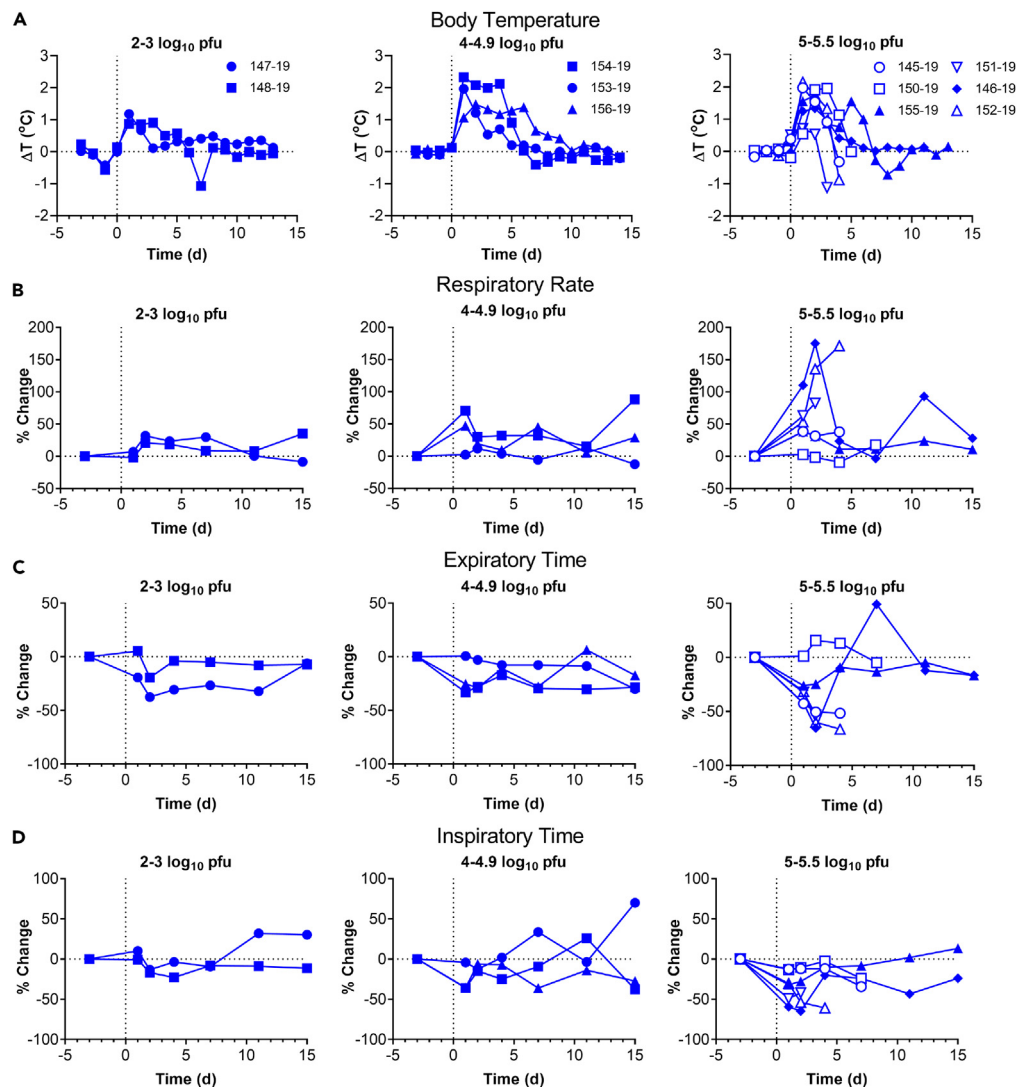
Figure 1. Fever and respiratory changes associated with H5N1-mediated disease in macaques

Macaques were infected with aerosolized H5N1 across a range of doses to understand the relationship between dose, disease, and outcome. Closed symbols are macaques that survived infection; open symbols are macaques that succumbed to infection.

(A) show daily median residual temperatures (difference between actual and predicted temperatures) as recorded by telemetry for individual macaques separated by dose range.

(B–D) changes in respiratory parameters measured by plethysmograph on days 2, 4, 7, 11, and 14. Graphs show percent change from baseline in (B) respiratory rate, (C) expiratory time, and (D) inspiratory time.

exposed to 5–5.5 $\log_{10}$ pfu had pronounced elevation in respiratory rates at 1 day post-infection which elevated further at day 2 in three macaques, recapitulating what we had reported previously with higher dose (>6 $\log_{10}$ pfu) challenge (Figure 1B).[25] There were corresponding drops in expiratory time and inspiratory time for five of the six macaques at doses between 5 and 5.5 $\log_{10}$ pfu (Figures 1C and 1D, right graphs). Serum samples taken at study endpoint confirmed that all surviving macaques had been infected with H5N1 as they had seroconverted for influenza viral nucleoprotein (Figure S3). Together, we found that influenza-associated ARDS and fatality are reproducibly induced in macaques with an aerosolized HPAI H5N1 infection at inhaled doses as low as 5 $\log_{10}$ pfu.

Markers associated with severe disease and determination of half-maximal lethal dose

Since we have cohorts of macaques that developed severe and non-severe disease in this study, we sought to identify markers that were associated with severe disease to better characterize the model. Figure 2 shows those biomarkers which correlated best with the inhaled dose of H5N1. There was a trend toward a higher average elevation in body temperature at the higher challenge doses tested (Figure 2A). At doses ranging 5–5.5 $\log_{10}$ pfu, there is also a trend toward higher average body temperature elevation in macaques that succumbed
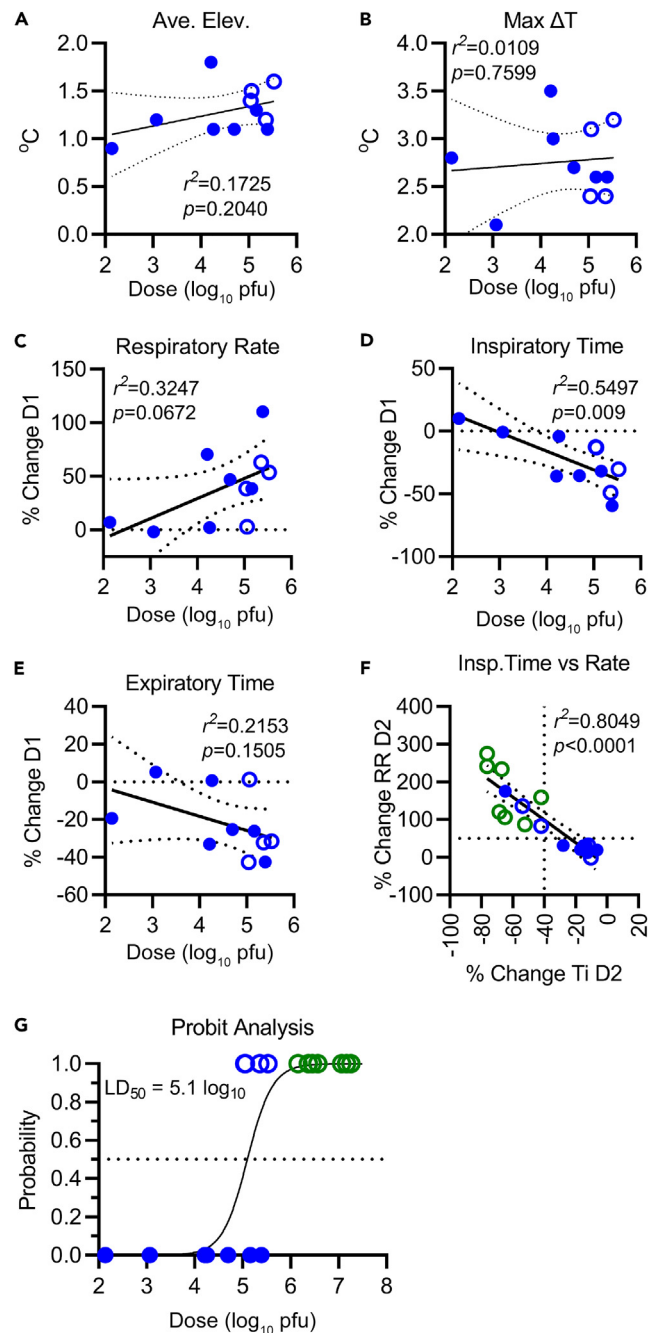
Figure 2. Correlation of H5N1 inhaled dose with respiratory disease and outcome

Closed symbols are macaques that survived infection; open symbols are macaques that succumbed to infection.

(A–F) Graphs show relationship between inhaled virus dose (x axis) with (A) average elevation in body temperature; (B) maximum deviation in body temperature; (C) respiratory rate on day 1; (D) inspiratory time on day 1; (E) expiratory time on day 1. (F) shows the correlation in the percent change in day 2 respiratory rate (RR) and inspiratory time (Ti) using macaques from this study (blue circles) as well as the original pilot study (green circles); the solid line is the linear regression analysis and dotted lines show the 95% confidence intervals.

(G) logistical regression analysis of dose and outcome of aerosol H5N1 infection in macaques to determine the LD_{50}.

compared to survivors although, given the small numbers, this trend was not statistically significant. Maximum deviation in temperature did not correlate with inhaled virus dose (Figure 2B). Linear trends correlated with challenge dose emerge at day 1 for all respiration parameters. Respiration rate increases and both inspiratory time and expiratory time decrease with increasing dose (Figures 2C–2E, respectively), although only the decrease in inspiratory time is statistically significant. Inspiratory time significantly decreased with increased respiratory
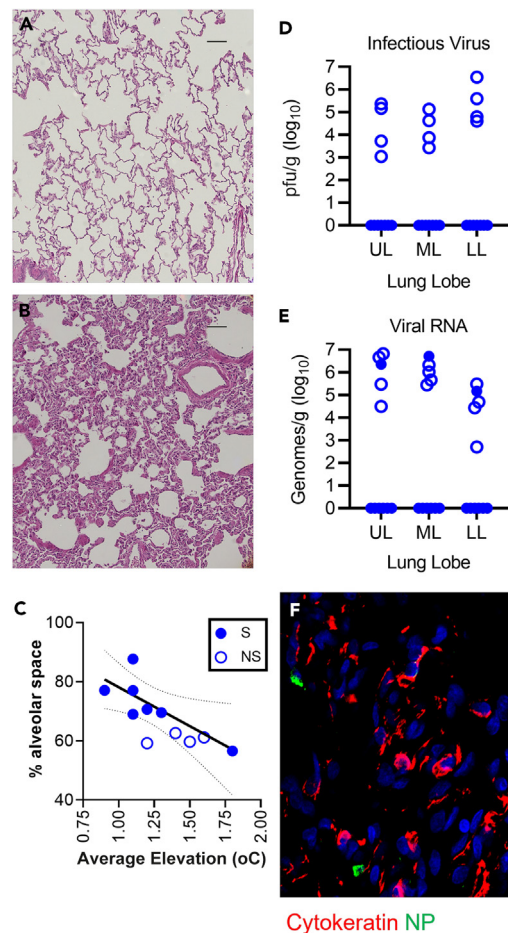
Figure 3. Pathological changes and viral load in the lungs

(A and B) 20× magnification of hematoxylin and eosin staining of lung sections from two macaques that survived H5N1 challenge, (A) macaque 147-19, which survived with only mild disease, (B) macaque 154-19 which had severe respiratory disease but survived. Scale bar is 100 µm.

(C) Graph in (C) shows percent alveolar space (y axis) with average temperature elevation (x axis); survivors (S) are plotted as solid circles; non-survivors (NS) are open circles. Lines show the linear regression analysis of survivors with the 95% confidence intervals.

(D and E) viral load in the lung at necropsy; macaques that survived are plotted as solid circles; non-survivors are open circles. UL = upper right lung; ML = middle right lung; LL = lower right lung. (D) infectious virus as measured by plaque assay of lung tissues; (E) viral RNA as measured by qRT-PCR of lung tissues.

(F) Expression of viral nucleoprotein (green) with that of cytokeratin (red) in the lung of 154-19, a macaque that survived severe H5N1 infection (400× magnification).

rate (Figure 2F). Although changes at day 2 in respiratory rate, inspiration time, and expiratory time were more severe, especially at the higher dose levels, the linear correlation with challenge dose was not as strong (Figure S2). A linear trend of decreased tidal volume with increasing challenge dose appears at day 1 and is statistically significant at day 2 (Figure S2). Using data from macaques in this study as well as our previous study,[25] at day 2 post-infection, nine of ten macaques that succumbed to H5N1-induced ARDS had a $\geq$40% decrease in inspiratory time and $\geq$50% increase in respiratory rate, while only one out of seven macaques that survived had respiratory changes that severe (Figure 2F). Combining the survival data from this dose study and the previous study,[25] probit analysis estimated the lethal dose 50 (LD_{50}) to be 5.1 log_{10} pfu. (Figure 2G). Hence, we established a severe respiratory disease model using cynomolgus macaques and determined the 50% lethal dose of aerosolized HPAI H5N1 virus in this model.

Pathological and virological changes in lung associated with dose and severe disease

Hematoxylin and eosin staining of macaque lungs showed relatively normal lung architecture in macaques that survived to the study endpoint (day 15) after mild disease (Figure 3A), whereas there was a considerable influx of leukocytes and edema in a surviving macaque (154-19) that developed severe disease (Figure 3B). ImageJ software was used to analyze changes in alveolar space of macaques infected with H5N1 virus. Among surviving macaques, loss of alveolar space correlated with the average elevation in body temperature (r^2 = 0.6136; p = 0.0372; Figure 3C). All four macaques that succumbed had comparably lower (~60%) alveolar space and a > 1°C average elevation in body temperature.

Binding Antibody

Neutralizing Antibody
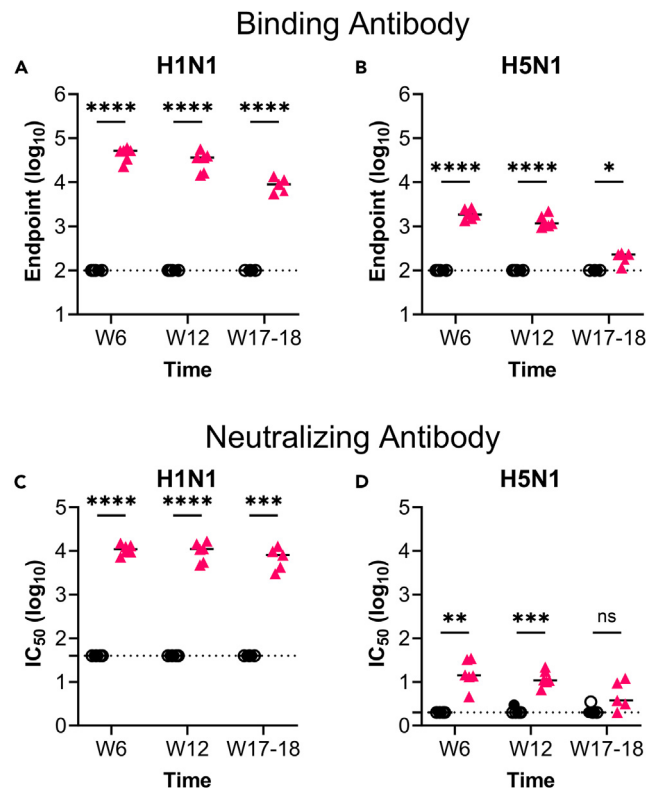
Figure 4. Humoral response elicited by aQIV vaccination against both H1N1 and H5N1

(A–D) (A) anti-H1N1 IgG endpoint titer as measured by ELISA from sera samples collected prior to challenge; (B) anti-H5N1 IgG endpoint titer as measured by ELISA from sera samples collected prior to challenge; (C) neutralizing activity against H1N1 in sera as measured by PRNT; (D) neutralizing activity against H5N1 in sera as measured by PRNT. Black circles are mock-vaccinated macaques; red triangles are aQIV-vaccinated macaques. Solid lines indicate the median. Dotted lines indicate lowest dilution of serum tested. *$p < 0.05$, ***$p = 0.0001$, ****$p < 0.0001$, n.s. = not significant by mixed-effects analysis.

Infectious virus was found in the lungs of all four macaques that succumbed, with titer varying from 3–6.5 $\log_{10}$ pfu/g (Figure 3D). Among macaques that survived infection, no infectious virus was found by plaque assay. This was likely due to the late sampling time point (day 15). One surviving macaque (154-19) had detectable viral RNA in the lung; this macaque was in the 4–4.9 $\log_{10}$ pfu dose range but had the highest average elevation in body temperature among survivors and had the lowest percentage of alveolar space (Table 1; Figure 3C). Immunohistochemistry confirmed the presence of influenza nucleoprotein in the lungs of 154-19 at the time of euthanasia, although it is not clear whether live virus was still present (Figure 3F).

Adjuvanted QIV vaccination protects macaques against lethal aerosolized H5N1

Epidemiological data suggest that prior exposure to H1N1 virus may impact the outcome of infection with H5N1 virus (the hemagglutinin [HA] for both viruses belong to group 1),[7] but there has been no evaluation of the protection afforded by seasonal influenza vaccination on the outcome of H5N1 virus infection in humans. This would be difficult to assess in human populations because most adults have also had influenza infection at least once in their lifetime. In mice and ferrets, there was only negligible protection against H5N1 virus challenge after aQIV vaccination.[28] Cynomolgus macaques, however, are phylogenetically closer to humans and are outbred, and efficacy in this model might be more translatable to humans. To test whether antigenic contents within commercial influenza vaccines could confer protection from mortality and/or morbidity in the aerosolized H5N1 infection macaque model, six macaques were vaccinated with three doses of aQIV, QIV adjuvanted with AddaVax, a squalene-based oil-in-water emulsion similar to MF59,[29] at 0, 4, and 10 weeks. The choice of adjuvant, doses, and schedule were identical to those in our prior influenza vaccine studies in macaques.[30,31] A second group of six macaques served as controls and were not vaccinated. Vaccinations were staggered such that two macaques would be challenged at a time, maintaining the time between vaccination and challenge but allowing for optimal collection of samples post-challenge, particularly at necropsy (see Table S1; Figure S4). Blood samples were collected at 2 weeks after second and third aQIV immunization (week 6 and 12, respectively) and 7 days prior to H5N1 challenge (week 17–18 post-vaccination) for analysis of the humoral response. All aQIV-vaccinated macaques were positive for antibody which bound HA of H1N1 and H5N1 by ELISA at all time points tested though titers waned by 17–18 weeks post-vaccination. Statistical significance is noted at all time points when compared to titers in controls (Figures 4A and 4B). Control macaques had no detectable HA-binding antibody against either H1N1 or H5N1 by ELISA, so the endpoint titer shown is the lowest dilution tested.

Table 2. Challenge doses, outcome, and febrile responses after aerosol challenge of control and aQIV-vaccinated macaques with lethal H5N1

Group	Animal ID	Dose[a]	TTD[b]	Fever			
				ΔT Max[c]	Duration[d]	Severity[e]	Ave Elev[f]
Control	290-20	5.58	4	2.78	57.25	98.93	1.73
	295-20	5.67	15	3.39	147.50	253.91	1.72
	308-20	5.93	4	3.59	77.25	156.58	2.03
	311-20	5.38	3	3.69	64.75	145.71	2.25
	25-21	5.60	3	3.40	60.50	127.61	2.11
	26-21	6.41	15	2.98	157.00	201.09	1.28
	Median	5.63	4.00	3.40	71.00	151.14	1.88
aQIV	291-20	5.40	15	2.98	98.50	158.01	1.60
	292-20	5.74	15	2.97	119.50	170.53	1.43
	307-20	6.09	15	2.83	111.00	174.04	1.57
	309-20	5.65	15	2.52	99.00	126.17	1.27
	24-21	5.99	15	3.16	119.50	145.83	1.22
	21-21	5.33	15	2.83	117.00	134.41	1.15
	Median	5.70	15.00	2.90	114.00	151.92	1.35

[a]Dose = inhaled dose, in log10 pfu.
[b]TTD = time to death.
[c]ΔTmax = maximum deviation from predicted temperatures.
[d]Duration = hours of significant temperature deviation from predicted.
[e]Severity = sum of significant temperature deviations, adjusted to hours.
[f]Ave Elev = average elevation in temperature, the product of dividing Severity by Duration.

aQIV-vaccinated macaques had strong serum neutralizing antibody titers against H1N1 virus at all three time points tested, with only minimal decline prior to challenge (Figure 4C). There was detectable neutralizing activity against H5N1 virus in the serum in all of the aQIV-vaccinated macaques at 6- and 12-week time points, although the titer was ~3 logs lower than what was measured for H1N1 virus (Figure 4D). At one week prior to challenge (week 17–18), neutralizing activity to H5N1 virus in aQIV-vaccinated macaques was no longer significantly different from the titers seen in controls but was overall higher than what was detected in controls. Control macaques had no detectable neutralizing antibody at any time point tested for H1N1 or H5N1 virus (Figures 4C and 4D).

Eight to nine weeks after the final vaccination (week 18–19), macaques were challenged with aerosolized H5N1 virus. Post-aerosol back-titration of the aerosol samples collected in all-glass impingers during the exposures indicates that the median dose achieved was 5.7 $\log_{10}$ pfu (4 × LD_{50}); there was some variation between individual macaques, but the difference between groups was not significant (median 5.63 vs. 5.70 $\log_{10}$ pfu for control and aQIV-vaccinated, respectively) (Table 2). Four of the six control macaques (67%) succumbed to H5N1 challenge before reaching study endpoint (15 days post-challenge), while all of the aQIV-vaccinated macaques survived (Table 2; Figure 5A). Macaques in both groups developed a fever within 24 h of infection although the median daily change in body temperature was lower in the aQIV-vaccinated group (Figure 5B). The change in respiratory rate was also substantially lower in aQIV-vaccinated macaques over the course of the post-exposure period, particularly if compared to control macaques that succumbed (Figure 5C). Using the criteria established for severe disease in the refinement of the model (inspiratory time <40% of baseline, respiratory rate >50% above baseline, see Figure 2F), at 2 days post-challenge all but one control and one aQIV-vaccinated macaques met the criteria for severe disease (Figure 5D). Similar to what we had seen in the model refinement, there was a strong association between change in respiratory rate and inspiratory time ($r^2 = 0.7841$; $p = 0.0001$) and surviving macaques were the least affected. Both average elevation in temperature ($p = 0.0193$) and maximum deviation in temperature ($p = 0.0359$) were significantly different between control macaques and aQIV-vaccinated macaques (Figure 5E). The percent change in respiratory rate at day 2 was high in both controls and aQIV-vaccinated macaques, and the difference was not statistically significant ($p = 0.0770$). Viral titer in bronchoalveolar lavage (BAL) on day 4 was significantly lower in aQIV-vaccinated macaques compared to controls ($p = 0.0001$). Serial chest plain radiographs revealed areas of airspace opacities consistent with acute pneumonia and edema in most of the macaques in both groups (Figures 5F and S5). Radiographic scores varied among macaques, and there was no statistical difference between groups (Figures S5C and S5D).

We compared antibody titer and reduction in disease across both groups, to see if antibody to H5N1 elicited by aQIV could correlate with a reduction in disease. H5N1 neutralizing activity at week 6 of vaccination correlated strongly with a reduction in virus titer in the BAL on day 4 post-challenge ($r^2 = 0.8409$; $p < 0.0001$) (Figure 5G). There was also a good correlation between the average elevation in body temperature post-challenge and H5N1 neutralizing activity at week 6 ($r^2 = 0.5221$; $p = 0.0079$). The change in respiratory rate at day 2 did not correlate with H5N1 neutralizing activity at week 6 ($r^2 = 0.1924$; $p = 0.1538$) although there is a trend toward reduced respiratory rates with higher neutralizing antibody titer. This demonstrates that repeated immunizations with aQIV could elicit cross-reactive immunity against H5N1 that conferred protection from mortality but not morbidity in macaques after a semi-lethal dose of aerosolized H5N1 challenge.
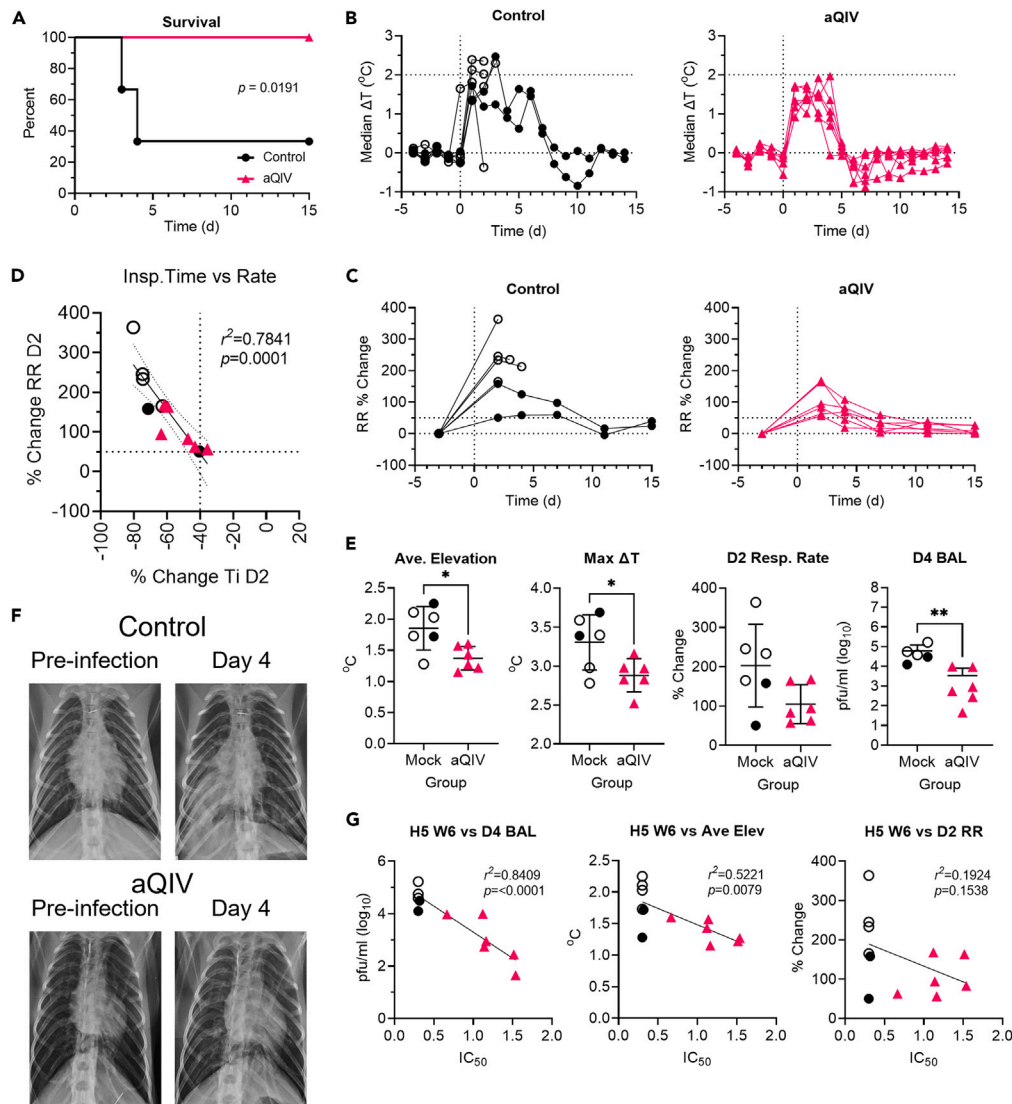
Figure 5. aQIV protects against death but not severe respiratory disease after lethal aerosol H5N1 challenge

(A) Survival after challenge over 15 days; (B–E), (G) black lines & circles denote mock-vaccinated macaques and red lines & triangles denote aQIV-vaccinated macaques; open symbols are macaques that succumbed to infection.

(B–G) (B) Median daily deviation in body temperature from predicted for mock-vaccinated (left graph) and aQIV-vaccinated (right graph) macaques; (C) % change in respiratory rate compared to baseline from predicted for mock-vaccinated (left graph) and aQIV-vaccinated (right graph) macaques; (D) Day 2 post-challenge change in inspiratory time (x axis) vs. respiratory rate (y axis) for all macaques; the solid line is the linear regression analysis and dotted lines show the 95% confidence intervals; (E) differences between mock-vaccinated and aQIV-vaccinated macaques in average temperature elevation, maximum temperature deviation, respiratory rate at day 2, and viral titer in BAL at day 4; lines show the average and standard deviation for each group, *p < 0.05, **p < 0.01 by Welch's t test; (F) radiographs of representative mock-vaccinated and aQIV-macaques prior to challenge and at day 4 post-challenge; (G) correlation of H5N1-neutralizing antibody at week 6 post vaccination and changes in day 4 BAL virus titer, average body temperature elevation, and day 2 respiratory rate. The solid line is the linear regression analysis for each graph.

DISCUSSION

Sporadic yet recurring outbreaks in humans as well as frequent spillovers to mammalian species of HPAI H5N1 virus pose serious concerns for a potential influenza pandemic in the future. Efforts to develop vaccine candidates that provide broader protection against future pandemic influenza viruses are critical to protect global public health. Concomitantly, efforts to develop model systems capable of evaluating vaccine and drug candidates are also essential as efficacy against pandemic influenza cannot be evaluated in human clinical trials. Here, we validated the use of aerosol challenge with HPAI H5N1 virus in the cynomolgus macaque model as a surrogate for human pandemic influenza virus

infection associated with high morbidity and mortality and showed that repeated vaccination with aQIV could offer protection from mortality caused by H5N1 virus.

We had previously established that in cynomolgus macaques, high doses of aerosolized H5N1 induced a fulminant, lethal viral pneumonia.[25] Infection triggered a cytokine storm and activation of the inflammasome, triggering pyroptosis of alveolar epithelial cells and disruption of the epithelial barrier.[32] We sought to evaluate here whether lower doses would extend the disease course and alter the outcome. At the lowest doses tested we still saw evidence of infection and viral replication but only mild disease. We were able to establish an estimated LD_{50} for aerosolized H5N1; macaques infected around this dose developed severe respiratory disease and two-thirds succumbed to disease and were humanely euthanized within 4–6 days. Hence, a lower viral dose did not extend the disease course substantially but resulted in comparatively milder disease within the same time frame. In recent years, two other groups have reported exposing macaques and marmosets to H5N1 via aerosol that did not result in lethal disease.[33–35] Although they used the same strain of H5N1 as was used in this study and in our prior study, these groups used different nebulizers than we did for aerosol generation and utilized a face mask to deliver aerosol as opposed to a head-only chamber. In further contrast to our methodologies, they did not sample the aerosols generated during the exposure. Consequently, the dose that was delivered to the lungs of the nonhuman primates in those studies is unknown. Comparing their data with the data we report here, the clinical signs they reported would be most consistent with an inhaled dose $<5 \log_{10}$ pfu.

Although HA of the HPAI H5N1 virus is quite different from that of seasonal human H1N1 viruses, both H5 and H1 subtypes belong to group 1 HAs, and there are conserved epitopes between these HAs including the stem region. Current seasonal influenza vaccines did not elicit protective immunity against lethal H5N1 challenge in mice or ferrets even when co-administered with adjuvant multiple times,[28] potentially due to the inability of these animals to efficiently respond to the HA stem epitope which is conserved among group 1 HA subtypes. In contrast, macaques are capable of generating neutralizing antibodies targeting the HA stem epitope,[30,31] and those antibodies could provide prophylactic protection against H5N1 in mice.[28,31] In this study, we showed that the aQIV-vaccinated macaques were protected against mortality caused by the aerosolized H5N1 infection. H5N1 virus neutralizing antibody titers did correlate with a reduction in both fever and virus titer in BAL. Given the weak neutralizing and HA-binding antibody titers to H5N1, it is possible that T cell responses might also be playing a role for the level of protection seen, similar to what has been suggested for how ancestral SARS-CoV-2 vaccines still prevent hospitalization and death after infection with new variants that are poorly recognized by anti-spike antibodies.[36,37] Alternatively, immune responses to other non-HA antigens such as neuraminidase may be playing a role in the protection against death.

In summary, our refined semi-lethal aerosolized H5N1 macaque infection model will be useful not only to study the pathogenesis of this important virus but also to evaluate candidate vaccines and therapeutics. In the wake of the coronavirus pandemic and a new emphasis on pandemic preparedness, extension of this macaque model to explore virulence of other influenza subtypes/strains and efficacy of medical countermeasures should be a high priority.

Limitations of the study

There are significant differences between the vaccination of macaques in this study and the regimen used in humans, so it is difficult to directly extrapolate our findings. Macaques were vaccinated three times with aQIV within 2.5 months, which is not a vaccination schedule used in humans. In addition, most humans of age ≥5 years are not immunologically naive to circulating influenza viruses and have had recurrent boosting of adaptive immune responses by vaccination and/or exposure throughout their lives. Future studies will be needed to fully assess the impact of pre-existing influenza immunity and immunological imprinting on subsequent vaccine-elicited protective immunity to H5N1 or other pandemic influenza viruses. The HPAI H5N1 A/Vietnam/1203/2004 strain in our studies belongs to a different clade from currently circulating strains in avian species, and our results may or may not be fully applicable to those newer isolates. This needs to be explored to better understand the threat posed by these currently circulating viruses.

STAR★METHODS

Detailed methods are provided in the online version of this paper and include the following:

- KEY RESOURCES TABLE
- RESOURCE AVAILABILITY
  - Lead contact
  - Materials availability
  - Data and code availability
- EXPERIMENTAL MODEL AND STUDY PARTICIPANT DETAILS
  - Macaques
- METHOD DETAILS
  - Challenge virus
  - Virus sequencing
  - Vaccination
  - ELISA
  - Reporter virus microneutralization
  - Aerosol exposures

- ○ Telemetry
- ○ Plethysmography
- ○ Plaque assay
- ○ Quantitative RT-PCR
- ○ Alveolar space analysis
- ○ Immunohistochemistry
- ○ Anti-NP ELISA
- ● QUANTIFICATION AND STATISTICAL ANALYSIS

AUTHOR CONTRIBUTIONS

Conceptualization: B.S.G., M.K., S.B.B., & D.S.R.; Formal Analysis: K.C., D.S.R., & C.W.; Investigation: R.A.G., M.M., K.J.O., C.W., S.M.M., M.W., L.T., H.S., G.K., H.R., T.S., L.O., P.D.S.C., J.C., M.X., E.O., S.B.B., & D.S.R.; Resources: D.P.; Data Curation: D.S.R. & S.B.B.; Writing – Original Draft: D.S.R. & M.M.; Writing – Review & Editing: M.K., R.A.G., K.C., S.B.B., & D.S.R.; Visualization: S.B.B. & D.S.R.; Supervision: M.K., B.S.G., S.B.B., & D.S.R.; Project Administration: M.K., B.S.G., S.B.B., & D.S.R.; Funding Acquisition: M.K., B.S.G., S.B.B., & D.S.R.

DECLARATION OF INTERESTS

The authors declare that they have no competing interests or conflicts.

INCLUSION AND DIVERSITY

One or more of the authors of this paper self-identifies as an underrepresented ethnic minority in their field of research or within their geographical location.

REFERENCES

1. Beigel, J.H., Farrar, J., Han, A.M., Hayden, F.G., Hyer, R., de Jong, M.D., Lochindarat, S., Nguyen, T.K.T., Nguyen, T.H., Tran, T.H., et al. (2005). Avian influenza A (H5N1) infection in humans. N. Engl. J. Med. *353*, 1374–1385. https://doi.org/10.1056/NEJMra052211.

2. Shi, J., Zeng, X., Cui, P., Yan, C., and Chen, H. (2023). Alarming situation of emerging H5 and H7 avian influenza and effective control strategies. Emerg. Microbes Infect. *12*, 2155072. https://doi.org/10.1080/22221751.2022.2155072.

3. Schrauwen, E.J.A., Bestebroer, T.M., Rimmelzwaan, G.F., Osterhaus, A.D.M.E., Fouchier, R.A.M., and Herfst, S. (2013). Reassortment between Avian H5N1 and human influenza viruses is mainly restricted to the matrix and neuraminidase gene segments. PLoS One *8*, e59889. https://doi.org/10.1371/journal.pone.0059889.

4. Sorrell, E.M., Schrauwen, E.J.A., Linster, M., De Graaf, M., Herfst, S., and Fouchier, R.A.M. (2011). Predicting 'airborne' influenza viruses: (trans-) mission impossible? Curr. Opin. Virol. *1*, 635–642. https://doi.org/10.1016/j.coviro.2011.07.003.

5. Herfst, S., Schrauwen, E.J.A., Linster, M., Chutinimitkul, S., de Wit, E., Munster, V.J., Sorrell, E.M., Bestebroer, T.M., Burke, D.F., Smith, D.J., et al. (2012). Airborne transmission of influenza A/H5N1 virus between ferrets. Science *336*, 1534–1541. https://doi.org/10.1126/science.1213362.

6. Imai, M., Watanabe, T., Hatta, M., Das, S.C., Ozawa, M., Shinya, K., Zhong, G., Hanson, A., Katsura, H., Watanabe, S., et al. (2012). Experimental adaptation of an influenza H5 HA confers respiratory droplet transmission to a reassortant H5 HA/H1N1 virus in ferrets. Nature *486*, 420–428. https://doi.org/10.1038/nature10831.

7. Gostic, K.M., Ambrose, M., Worobey, M., and Lloyd-Smith, J.O. (2016). Potent protection against H5N1 and H7N9 influenza via childhood hemagglutinin imprinting. Science *354*, 722–726. https://doi.org/10.1126/science.aag1322.

8. Bissel, S.J., Wang, G., Carter, D.M., Crevar, C.J., Ross, T.M., and Wiley, C.A. (2014). H1N1, but not H3N2, influenza A virus infection protects ferrets from H5N1 encephalitis. J. Virol. *88*, 3077–3091. https://doi.org/10.1128/JVI.01840-13.

9. Rimmelzwaan, G.F., Kuiken, T., van Amerongen, G., Bestebroer, T.M., Fouchier, R.A., and Osterhaus, A.D. (2001). Pathogenesis of influenza A (H5N1) virus infection in a primate model. J. Virol. *75*,

6687–6691. https://doi.org/10.1128/JVI.75.
14.6687-6691.2001.

10. Muramoto, Y., Shoemaker, J.E., Le, M.Q.,
Itoh, Y., Tamura, D., Sakai-Tagawa, Y., Imai,
H., Uraki, R., Takano, R., Kawakami, E., et al.
(2014). Disease severity is associated with
differential gene expression at the early and
late phases of infection in nonhuman
primates infected with different H5N1 highly
pathogenic avian influenza viruses. J. Virol.
88, 8981–8997. https://doi.org/10.1128/JVI.
00907-14.

11. Shinya, K., Gao, Y., Cilloniz, C., Suzuki, Y.,
Fujie, M., Deng, G., Zhu, Q., Fan, S., Makino,
A., Muramoto, Y., et al. (2012). Integrated
clinical, pathologic, virologic, and
transcriptomic analysis of H5N1 influenza
virus-induced viral pneumonia in the rhesus
macaque. J. Virol. 86, 6055–6066. https://doi.
org/10.1128/JVI.00365-12.

12. Baskin, C.R., Bielefeldt-Ohmann, H., Tumpey,
T.M., Sabourin, P.J., Long, J.P., García-Sastre,
A., Tolnay, A.E., Albrecht, R., Pyles, J.A.,
Olson, P.H., et al. (2009). Early and sustained
innate immune response defines pathology
and death in nonhuman primates infected by
highly pathogenic influenza virus. Proc. Natl.
Acad. Sci. USA 106, 3455–3460. https://doi.
org/10.1073/pnas.0813234106.

13. Soloff, A.C., Bissel, S.J., Junecko, B.F., Giles,
B.M., Reinhart, T.A., Ross, T.M., and Barratt-
Boyes, S.M. (2014). Massive mobilization of
dendritic cells during influenza A virus
subtype H5N1 infection of nonhuman
primates. J. Infect. Dis. 209, 2012–2016.
https://doi.org/10.1093/infdis/jiu009.

14. Cillóniz, C., Shinya, K., Peng, X., Korth, M.J.,
Proll, S.C., Aicher, L.D., Carter, V.S., Chang,
J.H., Kobasa, D., Feldmann, F., et al. (2009).
Lethal influenza virus infection in macaques is
associated with early dysregulation of
inflammatory related genes. PLoS Pathog. 5,
e1000604. https://doi.org/10.1371/journal.
ppat.1000604.

15. Chutinimitkul, S., van Riel, D., Munster, V.J.,
van den Brand, J.M.A., Rimmelzwaan, G.F.,
Kuiken, T., Osterhaus, A.D.M.E., Fouchier,
R.A.M., and de Wit, E. (2010). In vitro
assessment of attachment pattern and
replication efficiency of H5N1 influenza A
viruses with altered receptor specificity.
J. Virol. 84, 6825–6833. https://doi.org/10.
1128/JVI.02737-09.

16. Nicholls, J.M., Bourne, A.J., Chen, H., Guan,
Y., and Peiris, J.S.M. (2007). Sialic acid
receptor detection in the human respiratory
tract: evidence for widespread distribution of
potential binding sites for human and avian
influenza viruses. Respir. Res. 8, 73. https://
doi.org/10.1186/1465-9921-8-73.

17. Nicholls, J.M., Chan, M.C.W., Chan, W.Y.,
Wong, H.K., Cheung, C.Y., Kwong, D.L.W.,
Wong, M.P., Chui, W.H., Poon, L.L.M., Tsao,
S.W., et al. (2007). Tropism of avian influenza
A (H5N1) in the upper and lower respiratory
tract. Nat. Med. 13, 147–149. https://doi.org/
10.1038/nm1529.

18. Watanabe, T., Shinya, K., Watanabe, S., Imai,
M., Hatta, M., Li, C., Wolter, B.F., Neumann,
G., Hanson, A., Ozawa, M., et al. (2011).
Avian-type receptor-binding ability can
increase influenza virus pathogenicity in
macaques. J. Virol. 85, 13195–13203. https://
doi.org/10.1128/JVI.00859-11.

19. van Riel, D., Munster, V.J., de Wit, E.,
Rimmelzwaan, G.F., Fouchier, R.A.M.,
Osterhaus, A.D.M.E., and Kuiken, T. (2006).
H5N1 Virus Attachment to Lower Respiratory

Tract. Science 312, 399. https://doi.org/10.
1126/science.1125548.

20. van Riel, D., Munster, V.J., de Wit, E.,
Rimmelzwaan, G.F., Fouchier, R.A.M.,
Osterhaus, A.D.M.E., and Kuiken, T. (2007).
Human and avian influenza viruses target
different cells in the lower respiratory tract of
humans and other mammals. Am. J. Pathol.
171, 1215–1223. https://doi.org/10.2353/
ajpath.2007.070248.

21. Dabisch, P.A., Xu, Z., Boydston, J.A.,
Solomon, J., Bohannon, J.K., Yeager, J.J.,
Taylor, J.R., Reeder, R.J., Sayre, P., Seidel, J.,
et al. (2017). Quantification of regional
aerosol deposition patterns as a function of
aerodynamic particle size in rhesus macaques
using PET/CT imaging. Inhal. Toxicol. 29,
506–515. https://doi.org/10.1080/08958378.
2017.1409848.

22. Bowen, L.E., Rivers, K., Trombley, J.E.,
Bohannon, J.K., Li, S.X., Boydston, J.A., and
Eichelberger, M.C. (2012). Development of a
murine nose-only inhalation model of
influenza: comparison of disease caused by
instilled and inhaled A/PR/8/34. Front. Cell.
Infect. Microbiol. 2, 74. https://doi.org/10.
3389/fcimb.2012.00074.

23. Miller, M.A., Stabenow, J.M., Parvathareddy,
J., Wodowski, A.J., Fabrizio, T.P., Bina, X.R.,
Zalduondo, L., and Bina, J.E. (2012).
Visualization of murine intranasal dosing
efficiency using luminescent Francisella
tularensis: effect of instillation volume and
form of anesthesia. PLoS One 7, e31359.
https://doi.org/10.1371/journal.pone.
0031359.

24. Gregg, R.W., Maiello, P., Borish, H.J.,
Coleman, M.T., Reed, D.S., White, A.G.,
Flynn, J.L., and Lin, P.L. (2018). Spatial and
temporal evolution of lung granulomas in a
cynomolgus macaque model of
Mycobacterium tuberculosis infection.
Radiol. Infect. Dis. 5, 110–117. https://doi.
org/10.1016/j.jrid.2018.08.001.

25. Wonderlich, E.R., Swan, Z.D., Bissel, S.J.,
Hartman, A.L., Carney, J.P., O'Malley, K.J.,
Obadan, A.O., Santos, J., Walker, R.,
Sturgeon, T.J., et al. (2017). Widespread Virus
Replication in Alveoli Drives Acute
Respiratory Distress Syndrome in Aerosolized
H5N1 Influenza Infection of Macaques.
J. Immunol. 198, 1616–1626. https://doi.org/
10.4049/jimmunol.1601770.

26. Bowling, J.D., O'Malley, K.J., Klimstra, W.B.,
Hartman, A.L., and Reed, D.S. (2019). A
Vibrating Mesh Nebulizer as an Alternative to
the Collison Three-Jet Nebulizer for
Infectious Disease Aerobiology. Appl.
Environ. Microbiol. 85, e00747-19. https://
doi.org/10.1128/AEM.00747-19.

27. Roy, C.J., and Pitt, M.L.M. (2012). Infectious
Disease Aerobiology: Aerosol Challenge
Methods. In Biodefense Research
Methodology and Animal Models, J.R.
Swearengen, ed. (CRC Press), pp. 65–80.

28. Boyoglu-Barnum, S., Ellis, D., Gillespie, R.A.,
Hutchinson, G.B., Park, Y.J., Moin, S.M.,
Acton, O.J., Ravichandran, R., Murphy, M.,
Pettie, D., et al. (2021). Quadrivalent influenza
nanoparticle vaccines induce broad
protection. Nature 592, 623–628. https://doi.
org/10.1038/s41586-021-03365-x.

29. Mbow, M.L., De Gregorio, E., Valiante, N.M.,
and Rappuoli, R. (2010). New adjuvants for
human vaccines. Curr. Opin. Immunol. 22,
411–416. https://doi.org/10.1016/j.coi.2010.
04.004.

30. Darricarrère, N., Qiu, Y., Kanekiyo, M.,
Creanga, A., Gillespie, R.A., Moin, S.M.,

Saleh, J., Sancho, J., Chou, T.H., Zhou, Y.,
et al. (2021). Broad neutralization of H1 and
H3 viruses by adjuvanted influenza HA stem
vaccines in nonhuman primates. Sci. Transl.
Med. 13, eabe5449. https://doi.org/10.1126/
scitranslmed.abe5449.

31. Moin, S.M., Boyington, J.C., Boyoglu-
Barnum, S., Gillespie, R.A., Cerutti, G.,
Cheung, C.S.F., Cagigi, A., Gallagher, J.R.,
Brand, J., Prabhakaran, M., et al. (2022). Co-
immunization with hemagglutinin stem
immunogens elicits cross-group neutralizing
antibodies and broad protection against
influenza A viruses. Immunity 55, 2405–
2418.e7. https://doi.org/10.1016/j.immuni.
2022.10.015.

32. Corry, J., Kettenburg, G., Upadhyay, A.A.,
Wallace, M., Marti, M.M., Wonderlich, E.R.,
Bissel, S.J., Goss, K., Sturgeon, T.J., Watkins,
S.C., et al. (2022). Infiltration of inflammatory
macrophages and neutrophils and
widespread pyroptosis in lung drive influenza
lethality in nonhuman primates. PLoS Pathog.
18, e1010395. https://doi.org/10.1371/
journal.ppat.1010395.

33. Watanabe, T., Iwatsuki-Horimoto, K., Kiso,
M., Nakajima, N., Takahashi, K., Jose da Silva
Lopes, T., Ito, M., Fukuyama, S., Hasegawa,
H., and Kawaoka, Y. (2018). Experimental
infection of Cynomolgus Macaques with
highly pathogenic H5N1 influenza virus
through the aerosol route. Sci. Rep. 8, 4801.
https://doi.org/10.1038/s41598-018-23022-0.

34. Mooij, P., Stammes, M.A., Mortier, D.,
Fagrouch, Z., van Driel, N., Verschoor, E.J.,
Kondova, I., Bogers, W., and Koopman, G.
(2021). Aerosolized Exposure to H5N1
Influenza Virus Causes Less Severe Disease
than Infection via Combined Intrabronchial,
Oral, and Nasal Inoculation in Cynomolgus
Macaques. Viruses 13. https://doi.org/10.
3390/v13020345.

35. Iwatsuki-Horimoto, K., Nakajima, N., Kiso, M.,
Takahashi, K., Ito, M., Inoue, T., Horiuchi, M.,
Okahara, N., Sasaki, E., Hasegawa, H., and
Kawaoka, Y. (2018). The Marmoset as an
Animal Model of Influenza: Infection With
A(H1N1)pdm09 and Highly Pathogenic
A(H5N1) Viruses via the Conventional or
Tracheal Spray Route. Front. Microbiol. 9,
844. https://doi.org/10.3389/fmicb.2018.
00844.

36. Wang, Q., Bowen, A., Valdez, R., Gherasim,
C., Gordon, A., Liu, L., and Ho, D.D. (2023).
Antibody Response to Omicron BA.4-BA.5
Bivalent Booster. N. Engl. J. Med. 388,
567–569. https://doi.org/10.1056/
NEJMc2213907.

37. Liu, J., Chandrashekar, A., Sellers, D., Barrett,
J., Jacob-Dolan, C., Lifton, M., McMahan, K.,
Sciacca, M., VanWyk, H., Wu, C., et al. (2022).
Vaccines elicit highly conserved cellular
immunity to SARS-CoV-2 Omicron. Nature
603, 493–496. https://doi.org/10.1038/
s41586-022-04465-y.

38. Mena, I., Nelson, M.I., Quezada-Monroy, F.,
Dutta, J., Cortes-Fernández, R., Lara-Puente,
J.H., Castro-Peralta, F., Cunha, L.F., Trovão,
N.S., Lozano-Dubernard, B., et al. (2016).
Origins of the 2009 H1N1 influenza pandemic
in swine in Mexico. Elife 5, e16777. https://
doi.org/10.7554/eLife.16777.

39. Grabherr, M.G., Haas, B.J., Yassour, M., Levin,
J.Z., Thompson, D.A., Amit, I., Adiconis, X.,
Fan, L., Raychowdhury, R., Zeng, Q., et al.
(2011). Full-length transcriptome assembly
from RNA-Seq data without a reference
genome. Nat. Biotechnol. 29, 644–652.
https://doi.org/10.1038/nbt.1883.

40. Kent, W.J. (2002). BLAT–the BLAST-like alignment tool. Genome Res. *12*, 656–664. https://doi.org/10.1101/gr.229202.

41. Li, H., and Durbin, R. (2009). Fast and accurate short read alignment with Burrows-Wheeler transform. Bioinformatics *25*, 1754–1760. https://doi.org/10.1093/bioinformatics/btp324.

42. Haas, B.J., Papanicolaou, A., Yassour, M., Grabherr, M., Blood, P.D., Bowden, J., Couger, M.B., Eccles, D., Li, B., Lieber, M., et al. (2013). De novo transcript sequence reconstruction from RNA-seq using the Trinity platform for reference generation and analysis. Nat. Protoc. *8*, 1494–1512. https://doi.org/10.1038/nprot.2013.084.

43. Bohannon, J.K., Honko, A.N., Reeder, R.J., Cooper, K., Byrum, R., Bollinger, L., Kuhn, J.H., Wada, J., Qin, J., Jahrling, P.B., and Lackemeyer, M.G. (2016). Comparison of respiratory inductive plethysmography versus head-out plethysmography for anesthetized nonhuman primates in an animal biosafety level 4 facility. Inhal. Toxicol. *28*, 670–676. https://doi.org/10.1080/08958378.2016.1247199.

44. Albe, J.R., Ma, H., Gilliland, T.H., McMillen, C.M., Gardner, C.L., Boyles, D.A., Cottle, E.L., Dunn, M.D., Lundy, J.D., O'Malley, K.J., et al. (2021). Physiological and immunological changes in the brain associated with lethal eastern equine encephalitis virus in macaques. PLoS Pathog. *17*, e1009308. https://doi.org/10.1371/journal.ppat.1009308.

45. Ma, H., Lundy, J.D., O'Malley, K.J., Klimstra, W.B., Hartman, A.L., and Reed, D.S. (2019). Electrocardiography Abnormalities in Macaques after Infection with Encephalitic Alphaviruses. Pathogens *8*. https://doi.org/10.3390/pathogens8040240.

STAR★METHODS

KEY RESOURCES TABLE

REAGENT or RESOURCE	SOURCE	IDENTIFIER
Antibodies		
anti-influenza A nucleoprotein	BEI Resources	Clone DPJY03
Mouse anti-pan cytokeratin	Abcam	clone AE1/AE3
mouse anti-human CD163	ThermoFisher/eBioscience	eBioGHI/61
goat anti-mouse IgG2a Alexa Fluor 647	ThermoFisher	A-21241
goat anti-mouse Alexa Fluor 546	ThermoFisher	A-11030
Bacterial and virus strains		
H5N1 (A/Vietnam/1203/2004)	Daniel Perez, University of Georgia	N/A
Biological samples		
Cynomologus macaque lung & bronchoalveolar lavage	This paper	N/A
Cynomolgus macaque plasma	This paper	N/A
Chemicals, peptides, and recombinant proteins		
TRIzol	Invitrogen	15-596-018
Critical commercial assays		
Anti-NP inhibition assay	Virusys	IAV207-2
RNA Clean and Concentrator	Zymo	R1018
Reliance One-Step Multiplex Supermix	BioRad	12010220
rowhead**Deposited data**		
Raw telemetry & plethysmography data	Available on request	N/A
Exported & analyzed telemetry & plethysmography data	Available on request	N/A
ELISA, qRT-PCR, PRNT, plaque assay data	Available on request	N/A
Aerosol exposure data	Available on request	N/A
Immunohistochemistry images & alveolar space analysis data	Available on request	N/A
rowhead**Experimental models: Cell lines**		
MDCK cells	ATCC	CCL-34
Experimental models: Organisms/strains		
Cynomolgus macaques, Mauritius origin	VRC	N/A
Oligonucleotides		
Influenza A primers and probes	BEI Resources	NR-15592
Software and algorithms		
Prism 9	GraphPad	https://www.graphpad.com/
Ponemah 6.5	Data Sciences International	http://datasci.com
Finepointe 2.8	Data Sciences International	http://datasci.com
MatLab 2020a	MatLab	https://www.mathworks.com/products/matlab.html
NIS-ElementsAR v5.30.01	Nikon	https://www.microscope.healthcare.nikon.com/products/software/nis-elements
ImageJ	NIH	https://imagej.nih.gov/ij/

Continued		
REAGENT or RESOURCE	SOURCE	IDENTIFIER
rowheadOther		
Temperature data analysis code	Reed Lab	https://github.com/ReedLabatPitt/ Reed-Lab-Code-Library
Quadrivalent influenza vaccine + Addavax	Quadrivalent influenza vaccine: Seqirus. Addavax: Invivogen	Quadrivalent influenza vaccine: Afluria 2018-19. Addavax: vac-adx-10

RESOURCE AVAILABILITY

Lead contact

Further information and requests for resources and reagents should be directed to and will be fulfilled by the lead contact, Douglas Reed dsreed@pitt.edu.

Materials availability

This study did not generate new unique reagents.

Data and code availability

- All data reported in this paper will be shared by the lead contact upon request.
- Code used for analysis of telemetry data is available at https://github.com/ReedLabatPitt
- Any additional information required to reanalyze the data reported in this paper is available from the lead contact upon request.

EXPERIMENTAL MODEL AND STUDY PARTICIPANT DETAILS

Macaques

Young adult cynomolgus macaques (Macaca fasicularis) of Mauritius origin were used in these studies, with weights ranging from 3.1-6.4 kg at time of challenge. All macaques used in the H5N1 dose study were female; all macaques used in the vaccine study were male. Prior to delivery, macaques were screened to ensure they were naïve for influenza using an anti-nucleoprotein (NP) ELISA assay described subsequently. Research was conducted in compliance with the Animal Welfare Act and other Federal statutes and regulations relating to animals and experiments involving animals and adheres to principles stated in the Guide for the Care and Use of Laboratory Animals, National Research Council, 1996. The facility where this research was conducted is fully accredited by the Association for Assessment and Accreditation of Laboratory Animal Care International. Prior to initiation of experiments, the work with animals described in this report was approved by the University of Pittsburgh's Institutional Animal Care & Use Committee (IACUC).

METHOD DETAILS

Challenge virus

The virus (H5N1 A/Vietnam/1203/2004) used in these studies was generated by one passage in eggs from the original reverse genetics stock provided by Dr. S. Mark Tompkins at the Department of Infectious Diseases, University of Georgia.[25] Virus propagation was carried out under BSL3 conditions at the University of Pittsburgh Regional Biocontainment Laboratory. Virus stock was amplified in 10-11 day-old embryonated specific pathogen free chicken eggs for 24 h. Allantoic fluid from inoculated eggs was clarified by centrifugation and aliquots stored at -80°C. Virus titer was determined in MDCK cells by plaque assay and expressed as pfu/ml. Virus was diluted in DMEM containing bovine serum albumin, HEPES buffer, penicillin/streptomycin, and trypsin immediately prior to aerosol exposure.[26] Prior to initiation of experiments, the work with this virus described in this report was approved by the University of Pittsburgh's Institutional Biosafety Committee (IBC), Biohazards Committee, and Department of Environmental Health & Safety.

Virus sequencing

RNA was extracted using a MagNA Pure LC RNA Isolation Kit – High Performance (Roche) from 100 μl of virus on the MagNaPure LC instrument (Roche). The influenza genome was amplified by MS-RT-PCR. The 25 μl MS-RT-PCR (Superscript III high-fidelity RT-PCR kit, ThermoFisher Co.) utilized 2.5 μl of RNA as a template, and the primer sequences and concentrations were as follows: Opti1-F1 5′-GTTACGCGCCAGCAAAAGCAGG-3′ (0.06 μM); Opti1-F2 5′-GTTACGCGCCAGCGAAAGCAGG-3′ (0.14 μM); Opti1-R1 5′-GTTAC GCGCCAGTAGAAACAAGG-3′ (0.2 μM). The cycling conditions were 55°C for 2 min, 42°C for 1 hr, 94°C for 2 min, 5 cycles (94°C for 30 s, 44°C for 30 s, 68°C for 3.5 min), followed by 26 cycles (94°C for 30 s, 55°C for 30 s, 68°C for 3.5 min) and a final extension of 68°C for 10 min. Amplification of the influenza genome was confirmed by analyzing the MS-RT-PCR products in 0.8% agarose gel. The amplicons obtained from MS-RT-PCRs were purified using 0.45× of Agencourt AMPure XP Magnetic Beads (Beckman Coulter) and eluted in 30 μl of

HyClone molecular biology water (Genesee Scientific). The eluate's concentration was measured using the Qubit dsDNA HS Assay kit (ThermoFisher) on the Qubit 3.0 fluorometer (ThermoFisher), and the amplicons were normalized to 0.2 ng/µl. Adapters were added by tagmentation using the Nextera XT DNA library preparation kit (Illumina) with 40% of the suggested final volume. The libraries were purified using 0.7× Agencourt AMPure XP Magnetic Beads, and the fragment size distribution was analyzed on the Agilent Bioanalyzer using the High Sensitivity DNA kit (Agilent). Subsequently, the samples were normalized to 4 nM and pooled. The pooled libraries were loaded at a concentration of 15 pM and sequenced using the MiSeq v2, 300 cycle reagent Kit (Illumina) in a paired-end fashion (150 × 2). Genome assembly was performed using a pipeline developed previously at Icahn School of Medicine at Mount Sinai by Harm Van Bakel.[38] Initially, Cutadapt was used to remove low-quality sequences and adapters from paired FastQ files. The inchworm component of Trinity[39] was used to perform an initial assembly, and viral contigs bearing internal deletions were identified by BLAT[40] mapping against nonredundant IRD reference sequences. Subsequently, the inchworm assembly was repeated to remove breakpoint-spanning kmers from the assembly graph, and the resulting contigs were oriented and trimmed to remove low-coverage ends and any extraneous sequences beyond the conserved IAV termini. Finally, assembly contigs and contiguity were assessed for all segments by mapping sequence reads back to the final assembly using Burrows-Wheeler Alignment.[41] For the H5 HA segments, we also performed *de novo* assembly using Trinity.[42] A comparison of the consensus sequence to publicly available A/Vietnam/1203/2004 (H5N1) sequences on the Influenza Research Database (http://www.fludb.org/) showed no amino acid changes in the virus seed and propagated stocks used in this experiment.

Vaccination

At weeks 0, 4, and 10, macaques were inoculated by intramuscular injection with 500 µl of Aluria Quadrivalent 2018-19 seasonal influenza vaccine (Seqirus) and 500 µl of Addavax (Invivogen). Macaques in the control group were not inoculated. At various intervals post-vaccination and pre-challenge, macaques were bled and assessed for antibody response to influenza viruses by ELISA and reporter virus microneutralization assay.

ELISA

Macaque serum IgG levels were measured against recombinant HA of H1N1 (A/Michigan/45/2015) and H5N1 (A/Vietnam/1203/2004) by ELISA. Briefly, plates were coated with 2 µg/mL of recombinant HA proteins and incubated overnight at 4°C. Plates were washed with PBS and 0.1% Tween 20 after all incubations. Plates were blocked with 5% skim milk in PBS at 37°C for 1 h. Monoclonal antibodies and immune serum were serially diluted fourfold and plates were incubated for 1.5 h at 37°C. HRP conjugated secondary antibodies (anti-human; anti-monkey, Southern Biotech) were added and incubated for 1 hr at 37°C. Plates were developed with TMB substrate (KPL) and the reaction was stopped by the addition of 1 N H_2SO4. Absorbance was measured at 450 nm (Biotek Neo2 plate reader). ELISA endpoint titers were recorded as serum dilution resulting in 4-fold increase in OD_{450} value above the background.

Reporter virus microneutralization

Generation of the replication-restricted reporter (R3ΔPB1) virus H1N1 and rewired R3ΔPB1 (R4ΔPB1) virus H5N1 has been described elsewhere (Creanga, et al. Nat Commun. 2021). Briefly, to generate the R3/R4ΔPB1 viruses the viral genomic RNA encoding functional PB1 was replaced with a gene encoding the fluorescent protein (TdKatushka2), and the R3/R4ΔPB1 viruses were rescued by reverse genetics and propagated in the complementary cell line which expresses PB1 constitutively. Each R3/R4ΔPB1 virus stock was titrated by determining the fluorescent units per mL (FU/mL) prior to use in the experiments. For virus titration, serial dilutions of virus stock in OptiMEM were mixed with pre-washed MDCK-SIAT-PB1 cells (6 x 10^3 cells/well) and incubated in a 384-well plate in quadruplicate (25 µL/well). Plates were incubated for 18-26 h at 37°C with 5% CO_2 humidified atmosphere. After incubation, fluorescent cells were imaged and counted by using a Celigo Image Cytometer (Nexcelom) with a customized red filter for detecting TdKatushka2 fluorescence. For the microneutralization assay, serial dilutions of serum were prepared in OptiMEM and mixed with an equal volume of R3/R4ΔPB1 virus (~8 x 10^4 FU/mL). After incubation at 37°C and 5% CO_2 humidified atmosphere for 1 h, pre-washed MDCK-SIAT-PB1 cells (6 x 10^3 cells/well) were added to the serum-virus mixtures and transferred to 384-well plates in quadruplicate (25 µL/well). Plates were incubated and counted as described above. Target virus control range for this assay is 500 to 2,000 FU per well, and cell-only control is acceptable up to 30 FU per well. The percent neutralization was calculated for each well by constraining the virus control (virus plus cells) as 0% neutralization and the cell-only control (no virus) as 100% neutralization. A 7-point neutralization curve was plotted against serum dilutions for each sample, and a four-parameter nonlinear fit was generated using Prism (GraphPad) to calculate the 50% (IC_{50}) inhibitory concentrations.

Aerosol exposures

Aerosol exposures were performed under the control of the Aero3G aerosol management platform (Biaera Technologies, Hagerstown, MD) as previously described.[27] Macaques were anesthetized with 6 mg/kg Telazol® (Tiletamine HCl / Zolazepam HCl); once anesthesia was confirmed the macaque was weighed, bled, and transported to the Aerobiology suite using a mobile transport cart. The macaque was then transferred from the cart into a class III biological safety cabinet and the macaque's head was placed inside a head-only exposure chamber. Exposures were either time-calculated (using minute volume measured prior to exposure) or accumulated tidal volume-based (ATV). ATV exposures used Ponemah software (DSI; Data Sciences International, St. Paul, MN) measuring respiratory function via Jacketed External Telemetry Respiratory Inductive Plethysmography (JET-RIP; Data Sciences International, St. Paul, MN) belts that were placed around the

upper abdomen and chest of the macaque and calibrated to a pneumotach. This allowed monitoring and recording of respiratory function during the exposure via the Ponemah software platform (DSI) during the aerosol.[43] Tidal volume data was transferred from Ponemah via software interface with the Biaera software controlling the Aero3G; ATV exposures are terminated when the desired total inhaled volume of air has been reached (6 liters for these exposures). Aerosols were generated using an Aerogen Solo vibrating mesh nebulizer (Aerogen, Chicago, IL) as previously described, with a total airflow of 16 lpm of air into the chamber (one complete air change every 2 minutes).[26] Total exhaust from the chamber including sampling was equal to intake air. To determine inhaled dose, an all-glass impinger (AGI; Ace Glass, Vineland, NJ) was attached to the chamber at operated at 6 lpm, -6 to -15 psi. Particle size was measured once during each exposure at 5 minutes using an Aerodynamic Particle Sizer (TSI, Shoreview, MN). A 5-minute air wash followed each aerosol before the macaque was removed from the cabinet and transported back to its cage and observed until fully recovered from anesthesia. Virus concentration in nebulizer and AGI samples was assessed by plaque assay; inhaled dose was calculated as the product of aerosol concentration of the virus and the accumulated volume of inhaled air.[27]

Telemetry

Each macaque was implanted with a DSI PhysioTel Digital radiotelemetry transmitter (DSI Model No. M00) capable of continuously recording body temperature. Telemetry implants were implanted abdominally and the surgical site closed using skin sutures. During acquisition, data was transmitted from the implant to a TRX-1 receiver mounted in the room connected via a Communications Link Controller (CLC) to a computer running Ponemah v6.5 (DSI) software. Preexposure data collection began at least seven days in advance of infection. Data collected from Ponemah was exported as 15-minute averages into Excel files which were subsequently analyzed in MatLab 2019a as previously described.[44,45] Using pre-exposure baseline data, an auto-regressive integrated moving average (ARIMA) model was used to forecast body temperature assuming diurnal variation across a 24-hour period. The code is available at https://github.com/ReedLabatPitt/Reed-Lab-Code-Library. Residual temperatures were calculated as actual minus predicted temperatures. Upper and lower limits to determine significant changes were calculated as the product of 3 times the square root of the residual sum of squares from the baseline data. Maximum ΔT was the highest residual difference between actual and predicted body temperature after challenge. Fever duration was calculated in hours by dividing the number of significant elevations by 4. Fever severity was calculated as the sum of all significant elevations in body temperature, divided by 4 to get fever-hours. Average elevation was calculated by dividing fever severity by fever duration.

Plethysmography

Respiratory function was assessed in anesthetized animals using a head-out plethysmography chamber and pneumotach connected to a digital preamplifier run by Finepointe v2.8 software (DSI). For purposes of this study, we used a universal study modified to collect data similar to the chronic obstructive pulmonary disease (COPD) studies that Finepointe has established for whole-body plethysmography chambers. The chamber, pneumotach, and preamplifier were calibrated each morning before use. The NHP was laid prone in the chamber and the chamber sealed, with the head and neck emerging from the chamber through a latex dam which is secured around the neck. Once the chamber was sealed, the system was started for a few minutes to acclimate the system and ensure good data is being collected prior to initiation of data collection which was for three minutes. Data was analyzed within Finepointe or in Excel & GraphPad. Data shown is the average of the three minute collection period.

Plaque assay

To quantify viral load in tissue homogenate, BAL, and aerosol, samples were titered by standard plaque assay. Snap-frozen tissues were homogenized in media containing FBS using an Omni tissue homogenizer (Omni International). Samples were diluted serially 10-fold, then adsorbed onto 70-80% confluent monolayers of MDCK cells (American Type Culture Collection) in duplicate wells of either six- or 12-well tissue culture plates, and overlaid with agarose-containing media with added TPCK-trypsin. Plates were then incubated for 3 d at 37°C, 5 d at 37°C for tissues. All plates were then fixed in formaldehyde for 2-24 hours, then stained with .25 % crystal violet to visualize plaques.

Quantitative RT-PCR

Serum, BAL, or tissue homogenate was mixed with TRI Reagent (Ambion), and RNA was extracted using either a PureLink viral RNA/DNA extraction kit (Invitrogen) or RNeasy mini kit (Qiagen). The SuperScript III Platinum one-step quantitative RT-PCR kit (Invitrogen) was used for amplification of each RNA sample. Influenza A primers, probe, and cycling conditions used for quantitative RT-PCR were followed as described in BEI Resources product information sheet NR-15592. A standard curve was generated using 10-fold dilutions of RNA from virus stock of known titer. PCR was conducted on a QuantStudio 6 flex (Thermofisher).

Alveolar space analysis

Formaldehyde fixed tissues were paraffin embedded by the University of Pittsburgh McGowan Institute or the Biospecimen Core. Tissue sections were cut to 5 μm and mounted on positively charged glass slides. Standard regressive hematoxylin (Cat # MHS16-500ml) and eosin (Cat # E511-100) staining was used to stain for histopathology. Coverslips were placed on the slides promptly using a 1:1 xylene:toluene mixture as a mounting medium. Using an Olympus Provis microscope, images of stained lungs were captured at 10x for analysis. At least 5 images were

captured of the lungs from each macaque. Transmitted light was set at 9.0 and exposure time was kept consistent for all images. The microscope was white balanced, and a blank image was obtained to remove shading. NIS-ElementsAR v5.30.01 was used to remove background shading and scale images to 1.35 μm per pixel 47. Alveolar space analysis was performed using the open-source ImageJ software (https://imagej.nih.gov/ij/) and selecting the Alveolar Space Analysis option from the Macro's tab. Next, the images to be evaluated were opened and two regions of interest were selected for the alveolar space analysis. Summaries and results for each image were saved as Microsoft Excel files.

Immunohistochemistry

Frozen 6 μm thick lung sections of NHP lungs were permeabilized with Triton X-100 0.25% in 1x PBS for 10 minutes prior to being blocked with 5% host antibody serum. The following primary antibodies were added to the slides overnight at 4C: anti-influenza A nucleoprotein (clone DPJY03; BEI Resources), mouse anti-pan cytokeratin (clone AE1/AE3; Abcam), and mouse anti-human CD163 (eBioGHI/61/Thermofisher). The following secondary antibodies from Thermo Fisher Scientific were added to the slides for 30 minutes at 4C: goat anti-mouse IgG2a Alexa Fluor 647, goat anti-mouse Alexa Fluor 546. DAPI staining was used to identify cell nuclei, and slides were mounted in ProLong Diamond Antifade Mountant (Thermo Fisher Scientific) and subsequently viewed on an Olympus FluoView FV1000 confocal microscope. Controls used included: secondary only, no stain (blank), and matched isotype controls.

Anti-NP ELISA

Prior to challenge and at d 2 post-challenge, macaques were screened for influenza A nucleoprotein Abs using an anti-nucleoprotein (NP) inhibition ELISA assay (Virusys) as per the manufacturer's protocol. In brief, wells are coated with NP followed by incubation with experimental sera, a second incubation with detection antibody, washing six times, and finally addition of chromogen before reading the plate on a standard 96-well plate photometer at 450 nm. Absorbance values from experimental sera were compared with positive and negative controls and the amount of anti-NP present is calculated using the NP reduction index (1 – [delta sample absorbance / delta negative control absorbance]).

QUANTIFICATION AND STATISTICAL ANALYSIS

Statistical analyses were performed in GraphPad (version 9.5.1) and RStudio (version 2022.07.2). Time-to-event data were compared between groups using the log-rank test and the Kaplan-Meier method was used to plot survival curves. Survival times are censored at the pre-specified end of study day. Temperature and respiration data were analyzed using the t-test for two groups and ANOVA for more than two groups. Means and standard deviations are displayed in figures. Simple linear regression models were used to assess association between variables and 95% confidence bands are displayed. All p-values are from two-sided tests with a nominal 0.05 significance level. Assays performed in duplicate or triplicate were averaged within subject prior to comparisons. All observed data for variables and time points of interest are included in the analysis.